Asociación Argentina
de Mecánica Computacional

Mecánica Computacional Vol XXIX, págs. 4635-4659 (artículo completo)
Eduardo Dvorkin, Marcela Goldschmit, Mario Storti (Eds.)
Buenos Aires, Argentina, 15-18 Noviembre 2010

FROM THE COLLOCATION BOUNDARY ELEMENT METHOD TO A MESHLESS FORMULATION

Ney A. Dumont

Civil Engineering Department, Pontifical Catholic University of Rio de Janeiro, PUC-Rio, 22451-900 Rio de Janeiro, Brazil, dumont@puc-rio.br, http://www.civ.puc-rio.br

Keywords: Boundary elements, variational methods, meshless methods.

Abstract. The present developments rely on a consistent formulation of the conventional, collocation boundary element method with the aim to establish a computationally less intensive procedure, although not necessarily less accurate, for large-scale, two-dimensional and three-dimensional problems of potential and elasticity. One shows that both the double-layer and the single-layer potential matrices, **H** and **G**, respectively, whose evaluation requires dealing with singular and improper integrals, may be obtained in an expedite way that circumvents almost any numerical integration – except for a few regular integrals. Although both **H** and **G** are full populated, special solution schemes (not developed in the paper) may be conceived to dramatically decrease the storage allocation required in the iterative solution of the matrix system. The evaluation of results at internal points is also straightforward, as the fundamental solutions of the boundary element method may be assumed as the domain trial functions. The evaluation of results takes into account boundary-layer effects, although special domain functions should be required to adequately simulate stress gradients related to notches and cracks. The paper focuses on the mathematical fundamentals of the formulation. A few examples illustrate the applicability of the method and some convergence issues. Application to large scale problems shall be dealt with opportunely.

1 INTRODUCTION

The hybrid boundary element method (HBEM) was introduced in 1987 (Dumont, 1987, 1989) on the basis of the Hellinger-Reissner potential (Reissner, 1950), as a generalization of Pian's hybrid finite element method (Pian, 1964). The formulation requires evaluation of integrals only along the boundary and makes use of fundamental solutions (Green's functions) to interpolate fields in the domain. Accordingly, an elastic body of arbitrary shape may be treated as a single finite macro-element with as many boundary degrees of freedom as desired. In the meantime, the formulation has evolved to several application possibilities, including time-dependent problems, fracture mechanics, some special cases of non-homogeneous materials, and gradient elasticity (Dumont and Oliveira, 2001; Dumont, 2003; Dumont and Lopes, 2003; Dumont et al, 2004; Wagner et al, 2004; Dumont and Huaman, 2010). The original method makes use of a flexibility matrix $\mathbf{F}^*$, for which evaluation of integrals along the entire boundary is required. A simplified, although equally accurate, version of the HBEM was proposed about a decade ago (Dumont and Chaves, 2001). This simplified hybrid boundary element method (SHBEM) makes use of a displacement matrix $\mathbf{U}^*$ that is obtained directly from the fundamental solution, with which the time-consuming evaluation of $\mathbf{F}^*$ is circumvented. It is shown that, with the SHBEM, the evaluation of the single-layer potential matrix $\mathbf{G}$ of the conventional, collocation boundary element method (CBEM) is also no longer necessary. The double layer potential matrix $\mathbf{H}$ of the CBMs is an integrant part of both the HBEM and the SHBEM (Dumont, 2010a). The present paper proposes a still more simplified version of the SHBEM, in which the coefficients of the matrix $\mathbf{H}$ may also be obtained with almost no need of integration. For this sake, one resorts to a matrix $\mathbf{T}^*$ of traction forces related to the fundamental solution of the problem (Dumont et al, 2009; Dumont and Oliveira, 2010). The method is adequate for large problems in the frequency-domain, for which a repetitive evaluation of matrix coefficients may be carried out more economically. The method is particularly applicable to problems that require complicated fundamental solutions, as for axisymmetric problems and in the gradient elasticity. The paper presents the concepts involved in this novel method and brings some numerical examples to assess its efficiency.

The formulations are presented for static problems and linear elastic isotropic materials, although the simplified proposition of the paper is particularly advantageous for problems involving time, eventual non-homogeneities and complicated fundamental solutions, in general. One introduces in Section 2 the basic equations of the problem. Section 3 presents the approximation possibilities of the numerical model in terms of displacements, traction forces and stresses. Section 4 deals with the consistent formulation of the conventional, collocation boundary element method (Dumont, 1998, 2010), with the adequate outline of the spectral properties of the matrices that make part of the formulation. The simplified hybrid boundary element method is outlined in Section 5 as briefly and objectively as possible. Finally, an expedite version of the simplified hybrid boundary element method is proposed in Section 6, which goes toward a meshless formulation. This expedite formulation is in fact a simplification of both the hybrid, variationally-based and the conventional boundary element methods - a conceptual unification of these methods. The formulation is completely justified in terms of virtual work statements and of linear algebra properties of the resultant matrices. An example of numerical applications to two-dimensional potential problems is shown in Section 7.

2 BASIC EQUATIONS OF ELASTOSTATICS

One is concerned with the three-dimension (3D) static, small displacement analysis of an elastic body. Potential problems as well as two-dimension (2D) elasticity problems are particular cases. Degenerated problems such as in the analysis of beams and plates require special equations of the continuum, but end up with similar nodal equations and similar matrix spectral relations. Problems dealing with symmetries and anti-symmetries are not directly comprised by the present developments, but may be taken into account with some minimal conceptual changes (Dumont and

Alves, 2002; Oliveira and Dumont, 2009). The present development is intended to be representative of a wide class of problems, including anisotropy, non-homogeneity, strain gradient elasticity, multifield materials and coupled problems, provided only that the fundamental solutions are available (Qin, 2007).

For notation conciseness, the arguments $\mathrm{x}, \mathrm{y}, \mathrm{z}$ of the functions are omitted, in general. Indicial notation is used, with subscripts i, j assuming values 1, 2 or 3, as referred to global coordinates $\mathrm{x}, \mathrm{y}, \mathrm{z}$, respectively. A subscript after a comma denotes derivative with respect to the corresponding coordinate direction. Repeated subscripts indicate summation. Arrays of constants are also referred to without subscripts, using bold-face, capital letters for matrices and bold-face, lower letters for vectors.

Let an elastic body be submitted to body forces b_i in Ω, to traction forces $\overline{t}_i$ on part Γ_σ of the boundary and to displacements $\overline{u}_i$ on the complementary part Γ_u.

The exact stress solution σ_{ij} of the elastic body satisfies the equilibrium equations

$$\left.\begin{array}{c} \sigma_{ji,j} + b_i = 0 \\ \sigma_{ji} = \sigma_{ij} \end{array}\right\} \quad \text{in} \quad \Omega \tag{1}$$

$$\sigma_{ji}\eta_j = \overline{t}_i \quad \text{on} \quad \Gamma_\sigma \tag{2}$$

where η_j are the cosine directors, the projections of the unit normal on Γ facing outward.

The exact displacement solution u_i satisfies the compatibility equation:

$$u_i = \overline{u}_i \quad \text{on} \quad \Gamma_u \tag{3}$$

Stresses and displacements are related by means of the elastic tensor C_{ijkl}:

$$\sigma_{ij} = C_{ijkl}\epsilon_{kl} \equiv C_{ijkl}u_{k,l} \tag{4}$$

In this equation, strains are defined for small displacements as $\epsilon_{kl} = \left(u_{k,l} + u_{l,k}\right)/2$. The elastic tensor is symmetric: $C_{ijkl} = C_{jikl}$ and $C_{ijkl} = C_{ijlk}$, as a result of the symmetry of both σ_{ij}, Eq. (1), and ϵ_{kl}; moreover, $C_{ijkl} = C_{klij}$, as obtained from the principle of superposition of effects (Betti's reciprocal theorem).

3 APPROXIMATE REPRESENTATION OF DISPLACEMENTS, STRESSES AND TRACTION FORCES

Several numerical models are developed in this paper with basis on different, although correlated, assumptions. In the following, one introduces approximation possibilities for displacements and traction forces along the boundary - initially without any reference to some specific numerical discretization method. A stress field representation in the domain is also proposed, which may play the role of either weighting functions or actual stress approximations, depending on the numerical model.

The displacements are approximated only along the boundary, in the frame of an *external* reference system, as nodal displacements together with equivalent nodal forces shall ultimately build up stiffness - or stiffness-like - matrices according to which boundary restrictions are imposed and the problem is solved. The boundary traction forces may also be approximated in terms of Lagrangian multipliers - from which comes the name in this paper of an *auxiliary* reference system. The stress field is modeled by means of fundamental solutions - with no relation to the boundary conditions. This is the reason why such a stress representation is referred to as in an *internal* system.

3.1 Boundary displacement and geometry approximation - the *external* reference system

The displacements u_i are approximated along Γ by u_i^d given as

$$u_i^d = u_{in} d_n \quad \text{on} \quad \Gamma \tag{5}$$

where u_{in} are polynomial interpolation functions with compact support and $\mathbf{d} = [d_n] \in \mathbb{R}^{n^d}$ are nodal displacement parameters. The superscript d denotes *displacement* approximation. The index i refers to the coordinate directions whereas the index n refers to any of the n^d displacement degrees of freedom of the problem (thus denoting both location and orientation), for nodes adequately distributed along the boundary Γ.

Evaluated at nodal points, the interpolation functions u_{in} present the property

$$u_{in} \equiv \delta_{in} \tag{6}$$

in terms of the generalized Kronecker delta:

$$\delta_{in} = \begin{cases} 1 & \text{if } i \text{ and } n \text{ refer to the same degree of freedom} \\ 0 & \text{otherwise} \end{cases} \tag{7}$$

Equation (5) holds along Γ_u, in particular, according to Eq. (3)

$$\overline{u}_i = u_{in} \overline{d}_n \quad \text{on} \quad \Gamma_u \tag{8}$$

where $\overline{d}_n$ are nodal values of $\overline{u}_i$.

Moreover, one introduces a matrix $\mathbf{W} = [W_{ns}] \in \mathbb{R}^{n^d \times n^r}$, whose columns form an orthogonal basis of the nodal displacements $\mathbf{d}$ of Eq. (5) related to rigid body displacements of the elastic body comprised by the closure of the finite domain Ω. The number n^r of rigid body displacements is equal to 3 or 6, for general 2D or 3D elasticity problems, respectively (or equal to 1, if particularized to potential problems); it depends on the specific problem under analysis and particularly on symmetry issues. $\mathbf{W}^{\mathrm{T}}\mathbf{W}$ is the identity matrix of order n^r, and $\mathbf{W}\mathbf{W}^{\mathrm{T}}$ is an idempotent matrix of order n^d and rank n^r. $\mathbf{W}\mathbf{W}^{\mathrm{T}}$ is invariant, i. e., it does not depend on particular choices of the normal basis $\mathbf{W}$. Rigid-body displacement functions u_{is}^r are defined in Ω and normalized in such a way that the values of u_{is}^r and W_{ns} coincide at the nodal points:

$$u_{is}^r = u_{in} W_{ns} \quad \text{on} \quad \Gamma \tag{9}$$

The boundary geometry is approximated from the nodal attributes using the same interpolation functions u_{in} of Eq. (5), which consists in an isoparametric representation of the problem, exactly as in the displacement finite element method.

3.2 Boundary traction-force approximation - an *auxiliary* reference system

As required in the conventional boundary element method, the traction forces t_i are approximated along Γ by t_i^t given as

$$t_i^t = u_{i\ell} \frac{\left|J\right|_{(at\,\ell)}}{\left|J\right|} t_\ell \quad \text{on} \quad \Gamma \tag{10}$$

where $u_{i\ell}$ are polynomial interpolation functions with compact support and $\mathbf{t} = [t_\ell] \in \mathbb{R}^{n^t}$ are traction-force parameters. The superscript t stands for *traction*-force approximation. The index i refers to the coordinate directions whereas the index ℓ refers to any of the n^t traction-force degrees

of freedom of the problem (thus denoting both location and orientation), for nodes adequately distributed along boundary segments of Γ. The interpolation functions $u_{i\ell}$ have the same properties of u_{in}, as presented in Eqs. (6) and (7). Eq. (10) holds as $\overline{t}_i = u_{i\ell}\overline{t}_\ell$ along Γ_σ, in particular, according to Eq. (2). Equation (10) introduces a novel, slight improvement, as compared with the traditional boundary element implementation: $|J|_{(at\,\ell)}$ is the value at the nodal point ℓ of the Jacobian of the global-to-natural coordinate transformation and the term $|J|_{(at\,\ell)}/|J|$ features a term in the denominator that cancels with the term of the infinitesimal boundary expression $\mathrm{d}\Gamma = |J|\,\mathrm{d}\xi\,\mathrm{d}\eta$. This simplifies the numerical integration of terms related to traction forces along curved boundary segments (Dumont, 2010b).

The numbers of degrees of freedom for traction forces n^t and displacements n^d are not necessarily the same, since one may need a sufficient number of traction-force parameters to represent traction discontinuities along the boundary, generally at nodes where adjacent boundary segments present different outward normals (Dumont, 2010). (The use of either double nodes or of discontinuous elements is deemed a conceptually inferior technique~\cite{Katori94}). Then, it results that $n^t \geq n^d$, in general, as t_ℓ in Eq. (10) are traction-force attributes on boundary segments, whereas d_n in Eq. (5) are displacement attributes at nodal points. (The latter are always uniquely evaluated at a nodal point, except in the particular case, not dealt with in the present outline, of the discretization of a crack tip.) The fact that $n^t \geq n^d$ leads to some rectangular matrices, which may be nevertheless dealt with adequately in the formulations to be outlined in Sections 4 and 7 (Oliveira, 2004}.

3.3 Field stress approximation in terms of fundamental solutions - the *internal* reference system

An approximate field stress solution σ_{ij}^s of the partial differential Eq. (1) is formulated as the superposition of two terms,

$$\sigma_{ij}^s = \sigma_{ij}^* + \sigma_{ij}^p = \sigma_{ijm}^* p_m^* + \sigma_{ij}^p \quad \text{in} \quad \Omega \tag{11}$$

The superscripts s, p and $*$ stand for *stress*, *particular* and *fundamental* solutions, respectively. The present assumption is primarily stated for a stress field, from which a displacement field is subsequently derived, as shown in the following, and initially applied as weighting functions, in Section 4.

In the above equation, σ_{ij}^p is an arbitrary particular solution of Eq. (1),

$$\sigma_{ji}^p{}_{,j} + b_i = 0 \quad \text{in} \quad \Omega \tag{12}$$

and σ_{ij}^* is expressed as a sum of homogeneous, *fundamental solutions*[1], such that

$$\sigma_{ji}^*{}_{,j} = \sigma_{jim}^*{}_{,j}\, p_m^* = 0 \quad \text{in} \quad \Omega \tag{13}$$

where $\mathbf{p}^* = [p_m^*] \in \mathbb{R}^{n^d}$ are force parameters and σ_{ijm}^* are fundamental solutions with global support and analytical in Ω, which are liable to be interpreted, depending on the context, as *weighting* functions, but also as *interpolation*, *approximation* or *trial* functions (the latter three adjectives are interchangeable). Although omitted in the paper, the arguments of the fundamental solutions are $(x - x_M, y - y_M, z - z_M)$, where (x_M, y_M, z_M) is the *source point* - at which the point force p_m^* is

[1] They are also called Green's functions, which are more precisely (usually singular) fundamental solutions chosen in such a way that some stress or displacement boundary conditions are satisfied as a premise. The denomination *fundamental solution* may be used in the widest sense, also applied to a non-singular solution.

applied - and (x, y, z) is the *field point* where the effect of p_m^* is evaluated.

It is worth remarking that the number of force parameters, n^d, is chosen - not coincidentally - as precisely the number of nodal displacement parameters d_n in Eq. (5). Moreover, the force parameters p_m^* of Eq. (11) are defined as point forces that may perform positive (virtual) work on the corresponding nodal displacement d_m of Eq. (5). This premise, borrowed from the traditional boundary integral developments, is crucial to the present outline.

Equation (13) leads to

$$\sigma^*_{jim},_j = 0 \quad \text{in} \quad \Omega \tag{14}$$

The fundamental solutions σ^*_{jim} are analytical in the domain of interest, but singular just outside Ω, more precisely at points of application of p_m^* distributed along Γ:

$$\sigma^*_{jim},_j + \Delta_{im} = 0 \quad \text{in} \quad \Omega_{ext} = \Omega \cup \Omega_0 \tag{15}$$

This is the usual expression found in the literature on boundary integral equations, except that, for clarification of concepts, one sometimes uses herein the extended domain $\Omega_{ext} = \Omega \cup \Omega_0$, where Ω_0 is understood as a set of infinitesimally small, closed regions containing each point of singularity. Δ_{im} is the pulse function, which has zero value everywhere in the domain, except for the vicinity of the point of application of p_m^*, where it tends to infinity, although with a finite value, when integrated over the open domain (see Figure 1). It is convenient (but not compulsory) to normalize Δ_{im}, as defined in the following.

For a domain Ω_{ext} comprising a singularity,

$$\int_{\Omega_{ext}} \Delta_{im} \mathrm{d}\Omega = \delta_{im} = \begin{cases} 1 & \text{if } i \text{ and } m \text{ refer to the same degree of freedom} \\ 0 & \text{otherwise} \end{cases} \tag{16}$$

with δ_{im} defined as in Eq. (7). Thus, p_m^* in Eq. (11) has the meaning of a unit point force applied at a nodal point on Γ, just outside Ω but infinitely close to it, with m characterizing both a geometric location and a direction. For problems of elasticity, σ^*_{jim} is the stress expression of Kelvin's solution (Brebbia et al, 1984), on which the conventional boundary element method relies. The similarity of representations of displacements u_i^d on Γ, with Eqs. (5) and (7), and of σ^*_{ij} in Ω, with Eqs. (11) and (16), is not a coincidence but rather a key concept that should deserve more explicit appreciation in the technical literature.

The elastic body is comprised by Ω, the actual domain of interest, and there is in principle no need to invoke the extension Ω_{ext}. The singularity explicitly expressed by Δ_{im} in Eq. (15) is a feature to be welcome not only in the frame of an integral statement but also in the present variational developments, as this will assure that the resulting equation systems are well conditioned.

The displacements corresponding to the stresses σ^s_{ij} are defined as

$$u_i^s = u_i^* + u_i^p + u_i^r = u^*_{im} p_m^* + u_i^p + u^r_{is} c_s \equiv (u^*_{im} + u^r_{is} C_{sm}) p_m^* + u_i^p \quad \text{in} \quad \Omega \tag{17}$$

where u_i^* and u_i^p are analytical displacement fields uniquely obtained - except for arbitrary rigid body displacements u_i^r - from the stress fundamental solution σ^*_{ij} given in Eq. (11) and from the body force particular solution σ^p_{ij} of Eq. (12), respectively. The vector of constants $\mathbf{c} = [c_s] \in \mathbb{R}^{n^r}$ is in principle arbitrary. The equivalent representation shown above, in terms of an arbitrary matrix of

constants $\mathbf{C}=[C_{sm}]\in\mathbb{R}^{n^d\times n^r}$ that multiplies $\mathbf{p}^*$, may become convenient in some of the following developments.

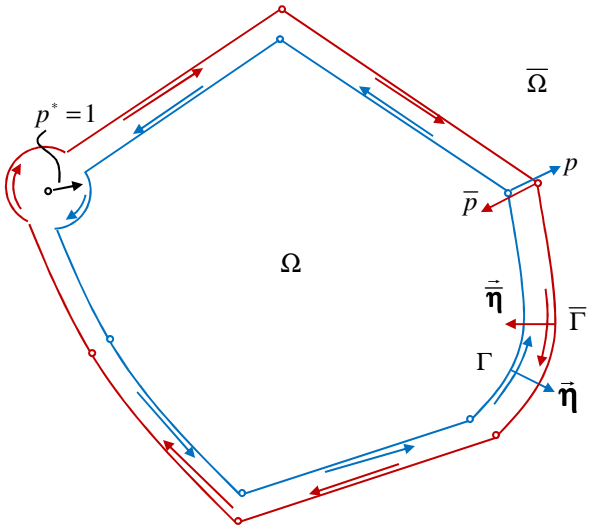

Figure 1: Scheme of a finite domain Ω and of the complementary, unbounded domain $\overline{\Omega}$, with respective integration orientations.

3.4 Some matrix relations that may become useful

Boundary approximation of the particular solution. As proposed for the sake of simplifying notation (Dumont, 2003), given a sufficiently refined boundary mesh, the displacements u_i^p and the traction forces t_i^p related to an arbitrary particular solution of the non-homogeneous governing Eq. (1), whenever available, can be approximated accurately enough by nodal displacement parameters $\mathbf{d}^p=[d_n^p]\in\mathbb{R}^{n^d}$ and traction force parameters $\mathbf{t}^p=[t_\ell^p]\in\mathbb{R}^{n^t}$, respectively, in terms of the interpolation functions of Eqs. (5) and (10):

$$u_i^p \approx u_{in} d_n^p \quad \text{on} \quad \Gamma \tag{18}$$

$$t_i^p \approx t_{i\ell} t_\ell^p \quad \text{on} \quad \Gamma \tag{19}$$

One assumes with the above equations that a particular solution for the domain forces b_i in Eq. (1) is known in terms of displacements u_i^p and stresses σ_{ij}^p. The means to obtain such particular solutions other than in close form are not discussed herein (see, for instance, Partridge et al, 1992).

Virtual-work representation of equivalent nodal forces. Moreover, it is sometimes advisable to think of the boundary traction forces as expressed in terms of equivalent nodal forces $\mathbf{p}=[p_m]\in\mathbb{R}^{n^d}$ that come up from the virtual work statement:

$$\begin{aligned} &\delta d_m p_m = \delta d_m \int_\Gamma u_{im} t_{i\ell} d\Gamma t_\ell \\ &\Rightarrow p_m = L_{\ell m} t_\ell \quad \text{or} \quad \mathbf{p}=\mathbf{L}^{\mathrm{T}}\mathbf{t} \end{aligned} \tag{20}$$

where $\mathbf{L}=[L_{\ell m}]\in\mathbb{R}^{n^t\times n^d}$, whose transpose performs an equilibrium transformation, is

$$\mathbf{L}\equiv L_{\ell m}=\int_\Gamma t_{i\ell} u_{im} d\Gamma \tag{21}$$

4 THE CONVENTIONAL BOUNDARY ELEMENT METHOD

The matrix equation of the conventional, collocation boundary element method (Brebbia et al,

1984) may be expressed from a minimum residual statement or, equivalently, directly from the Somigliana's identity in order to correlate boundary displacement and traction-force parameters d_n and t_ℓ, as introduced in Eqs. (5) and (10) under the premise of Eqs. (2) and (3), such that Eq. (1) is best satisfied:

$$\begin{aligned}&\delta p_m^* \left[\int_\Gamma \sigma_{jim}^* \eta_j u_{in} \mathrm{d}\Gamma - \int_\Omega \sigma_{jim}^*{}_{,j}\, u_{in} \mathrm{d}\Omega \right] d_n \\ &= \delta p_m^* \left[\int_\Gamma \left(u_{im}^* + C_{sm} u_{is}^r \right) t_{i\ell} \mathrm{d}\Gamma \right] t_\ell + \delta p_m^* \left[\int_\Omega \left(u_{im}^* + C_{sm} u_{is}^r \right) b_i \mathrm{d}\Omega \right]\end{aligned} \tag{22}$$

The weighting function is a virtual field that is in equilibrium in Ω, thus a variation of σ_{ij}^s in Eq. (11) expressed in terms of δp_m^*. The variation of the field displacements u_i^s in Eq. (17) also enters in the expression, which leads to two terms with the matrix C_{sm} of rigid body displacements. The presence of C_{sm} together with the use of the set of virtual forces δp_m^* make the above expression a consistent statement that is not usual in the literature (Dumont, 1998, 2010).

Since δp_m^* is arbitrary, Eq. (22) leads to the matrix expression

$$\mathbf{Hd} = \mathbf{Gt} + \mathbf{b} + \boldsymbol{\epsilon} \tag{23}$$

As it is developed in the sequence, this equation establishes displacement compatibility in terms of a set of equivalent nodal displacements $\mathbf{d}^* = [d_m^*] \in \mathbb{R}^{n^d}$ over which the force parameters $\mathbf{p}^*$ may perform virtual work, where $\mathbf{H} = [H_{mn}] \in \mathbb{R}^{n^d \times n^d}$ in the product $\mathbf{Hd}$ is a kinematic transformation matrix, $\mathbf{G} = [G_{m\ell}] \in \mathbb{R}^{n^d \times n^t}$ in the product $\mathbf{Gt}$ is a flexibility-like matrix (that is in general rectangular, as proposed) and $\mathbf{b} = [b_m] \in \mathbb{R}^{n^d}$ is a vector of nodal displacements equivalent to the applied body forces. The formal definition of these matrices is

$$H_{mn} = \int_\Gamma \sigma_{jim}^* \eta_j u_{in} \, d\Gamma \tag{24}$$

$$G_{m\ell} = \int_\Gamma t_{i\ell} u_{im}^* \, d\Gamma \tag{25}$$

$$b_m = \int_\Omega u_{im}^* b_i \mathrm{d}\Omega \tag{26}$$

$$\epsilon_m = \left[\int_\Gamma u_{is}^r t_{i\ell} \mathrm{d}\Gamma t_\ell + \int_\Omega u_{is}^r b_i \mathrm{d}\Omega \right] C_{sm} \tag{27}$$

The double-layer and single-layer potential matrices H_{mn} and $G_{m\ell}$ comprise in their definition singular and improper integrals, respectively, when source (m) and field (either n or ℓ) indexes refer to the same nodal points. Then, special care must be taken in the numerical integrations. If the integration of H_{mn} is represented as carried out along Γ_{ext}, in the frame of the outline presented with respect to Eqs. (15) and (16), a term δ_{mn} is naturally accrued (Dumont, 2010b). One is obviously taking into account the singularity present in Eq. (24), which presupposes adequate evaluation in terms of a Cauchy principal value. The representation of Eq. (24) is the simplest possible way, with any singularity being an issue to be dealt with mathematically.

The latter term in Eq. (23), as presented in Eq. (27), corresponds to residuals whose magnitude depends on the amount of rigid body displacements that are always implicit in the fundamental solution, Eq. (17), as well as on how refined the boundary has been discretized, that is, how accurately the boundary traction forces approximated according to Eq. (10) are in equilibrium with the applied domain forces b_i (then, the term in brackets is equal to zero only if the traction forces $t_{i\ell} t_\ell$ on Γ exactly reproduce the analytical solution of the problem). However, the vector of residuals $\boldsymbol{\epsilon}$ is usually disregarded in the implementations shown in the literature, or sometimes used as a measure of convergence of the numerical model. A consistent numerical model must take this

term explicitly into account (Dumont, 2010).

This specific issue has already been the subject of a thorough theoretical investigation (Dumont, 1998). The main results are briefly outlined in the following, also introducing a - not necessary, however convenient - simplification related to the particular solution term b_m of Eq. (26), as already alluded to with Eqs. (18) and (19).

The vector of residuals $\boldsymbol{\epsilon}$ in Eq. (27) may be written as

$$\boldsymbol{\epsilon} = \mathbf{C}^{\mathrm{T}}\mathbf{R}^{\mathrm{T}}\left(\mathbf{t}-\mathbf{t}^{p}\right) \tag{28}$$

where $\mathbf{R}=[R_{\ell s}]\in\mathbb{R}^{n^t\times n^r}$ is defined as

$$R_{\ell s} = \int_{\Gamma} u_{is}^{r} t_{i\ell}\,\mathrm{d}\Gamma l \tag{29}$$

and the product $\mathbf{R}^{\mathrm{T}}\mathbf{t}^{p}$ comes from the approximation

$$\int_{\Omega} u_{is}^{r} b_i\,\mathrm{d}\Omega = -\int_{\Gamma} u_{is}^{r}\sigma_{ji}^{p}\eta_j\,\mathrm{d}\Gamma \approx -\int_{\Gamma} u_{is}^{r} u_{i\ell}\,\mathrm{d}\Gamma t_{\ell}^{p} \tag{30}$$

whenever a particular solution for the body force problem, as stated in Eq. (12), is available. By the same token, the vector b_m of equivalent nodal displacements, introduced in Eq. (26), may be approximated as developed in the following:

$$b_m = \int_{\Omega} u_{im}^{*} b_i\,\mathrm{d}\Omega = -\int_{\Gamma} u_{im}^{*}\sigma_{ji}^{p}\eta_j\,\mathrm{d}\Gamma + \int_{\Gamma}\sigma_{jim}^{*}\eta_j u_i^{p}\,d\Gamma + \delta_{im}u_i^{p} \tag{31}$$

$$\Rightarrow b_m \approx -G_{m\ell}t_{\ell}^{p} + H_{mn}d_n^{p} \tag{32}$$

Then, making use of Eqs. (28) and (32), a convenient way of expressing Eq. (23) is

$$\mathbf{H}\left(\mathbf{d}-\mathbf{d}^{p}\right) = \left(\mathbf{G}+\mathbf{C}^{\mathrm{T}}\mathbf{R}^{\mathrm{T}}\right)\left(\mathbf{t}-\mathbf{t}^{p}\right) \tag{33}$$

One identifies in Eq. (28), as supported by other linear algebra manipulations (Dumont, 1998), that the columns of the matrix $\mathbf{R}$ span the space of inadmissible traction forces $\mathbf{t}-\mathbf{t}^{p}$ in Eq. (33) that cannot be transformed. Then,

$$\left(\mathbf{G}+\mathbf{C}^{\mathrm{T}}\mathbf{R}^{\mathrm{T}}\right)\mathbf{R}=\mathbf{0} \quad\Rightarrow\quad \mathbf{C}^{\mathrm{T}} = -\mathbf{G}\mathbf{R}(\mathbf{R}^{\mathrm{T}}\mathbf{R})^{-1} \tag{34}$$

which leads to the consistent boundary element equation

$$\mathbf{H}\left(\mathbf{d}-\mathbf{d}^{p}\right) = \mathbf{G}_a\left(\mathbf{t}-\mathbf{t}^{p}\right) \equiv \mathbf{G}\mathbf{P}_Z^{\perp}\left(\mathbf{t}-\mathbf{t}^{p}\right) \tag{35}$$

where $\mathbf{G}_a \equiv \mathbf{G}\mathbf{P}_Z^{\perp}$ is the *admissible* part of $\mathbf{G}$ and

$$\mathbf{P}_Z^{\perp} = \mathbf{I}-\mathbf{P}_Z = \mathbf{I}-\mathbf{R}(\mathbf{R}^{\mathrm{T}}\mathbf{R})^{-1}\mathbf{R}^{\mathrm{T}} = \mathbf{I}-\mathbf{Z}\mathbf{Z}^{\mathrm{T}} \tag{36}$$

is the orthogonal projector onto the admissible space of the traction forces, which comprises the subsets of tractions forces that are in balance and can therefore be transformed into equivalent nodal displacements. For the sake of convenience, one introduces the orthogonal basis $\mathbf{Z}$, such that $\mathbf{Z}^{\mathrm{T}}\mathbf{Z}=\mathbf{I}$, to represent the subspace spanned by the columns of $\mathbf{R}$. One observes that, from Eqs. (9) and (21),

$$\mathbf{R} = \mathbf{L}\mathbf{W} \tag{37}$$

which means that, from Eq. (20),

$$\mathbf{W}^{\mathrm{T}}\mathbf{p}=\mathbf{0} \quad\Leftrightarrow\quad \mathbf{R}^{\mathrm{T}}\mathbf{t}=\mathbf{0} \tag{38}$$

Moreover, one checks the consistency of Eq. (35) in terms of the spectral properties

$$\mathbf{W} = N(\mathbf{H}) \quad\Rightarrow\quad \mathbf{G}_a\mathbf{Z}=\mathbf{0} \tag{39}$$

whenever the elastic body is liable to rigid body displacements, which means that unbalanced traction forces are filtered from the compatibility equation. This is, however, not a fully consistent equation system, as the conventional boundary element method is not based on a variational principle and redundantly approximates via Eqs. (5) and (10) displacements and traction forces along Γ. This lack of full consistency is reflected by the fact that, given $\mathbf{V}$ as the null space of $\mathbf{H}^{\mathrm{T}}$,

$$\mathbf{V} = N(\mathbf{H}^{\mathrm{T}}) \quad \not\Rightarrow \quad \mathbf{V}^{\mathrm{T}}\mathbf{G}_a = 0 \tag{40}$$

in Eq. (35), although

$$\left|\mathbf{V}^{\mathrm{T}}\mathbf{G}_a\right| \to 0 \tag{41}$$

with increasing mesh refinement.

The inconsistent Eq. (23), obtained by just neglecting ϵ as usually presented in the literature, as well as the Eq. (33), in which one neglects $\mathbf{C}$, may be expressed as a compact system of equations in the shape

$$\mathbf{A}\mathbf{x} = \mathbf{y} \tag{42}$$

where the vector $\mathbf{x}$ gathers all the unknown coefficients of $\mathbf{d}$ and $\mathbf{t}$, $\mathbf{y}$ is a vector of known quantities and the (non-symmetric) square matrix $\mathbf{A}$ is obtained by adequately stacking the columns of $\mathbf{H}$ and $\mathbf{G}$ corresponding to the unknown coefficients. If one is lucky (as it seems to occur in the applications displayed in the literature), $\mathbf{G}$ is a full rank matrix and $\mathbf{A}$ is well conditioned. However, there is an in principle uncontrolled amount of rigid body displacements implicit in the term u^*_{im} of Eq. (42), so that the good conditioning of $\mathbf{A}$ cannot be assured beforehand (Rencis et al, 1995).

On the other hand, if one introduces the concept of an admissible matrix $\mathbf{G}_a$, as in Eq. (35), one assumes full control of the condition of $\mathbf{G}_a$: it is not full rank and $N\left(\mathbf{G}_a^{\mathrm{T}}\mathbf{G}_a\right) \approx \mathbf{V}$. This is auspicious news, since a singularity can be better handled than a quasi-singularity. However, one must prevent oneself from just trying to write Eq. (35) in the shape of Eq. (42), since now the matrix $\mathbf{A}$ would be definitely ill conditioned. On the other hand, if one adds to Eq. (35) the restriction that $\mathbf{R}\left(\mathbf{t}-\mathbf{t}^p\right)=\mathbf{0}$, according to Eq. (38), a system in the shape of Eq. (42) can be obtained and consistently solved in the frame of generalized inverse matrices.

4.1 Evaluation of a stiffness matrix

Instead of solving a problem in terms of the transformed system of Eq. (42), one may need to obtain a formulation in terms of a stiffness-type matrix,

$$\mathbf{K}\left(\mathbf{d}-\mathbf{d}^p\right)=\left(\mathbf{p}-\mathbf{p}^p\right). \tag{43}$$

The matrix $\mathbf{K}$ is obtained by solving for $\left(\mathbf{t}-\mathbf{t}^p\right)$ in Eq. (35) in terms of either $\mathbf{G}_a$ or $\mathbf{G}$, and also resorting to $\mathbf{L}^{\mathrm{T}}$ defined in eqn (24). A first possibility is

$$\mathbf{K}_{inconsistent} = \mathbf{L}^{\mathrm{T}}\mathbf{L}\left(\mathbf{G}\mathbf{L}\right)^{-1}\mathbf{H}, \tag{44}$$

where $\mathbf{L}\left(\mathbf{G}\mathbf{L}\right)^{-1}$ is a {1, 2, 3}-inverse of $\mathbf{G}$ ($\mathbf{G}\mathbf{L}$ supposedly well conditioned). There are several other possibilities, also in terms of a {1, 2, 3, 4}-inverse of $\mathbf{G}$ (Oliveira, 2004).

However, the only fully consistent formulation stemming from Eq. (35) is

$$\mathbf{K}_{consistent} = \mathbf{L}^{\mathrm{T}}\mathbf{P}_R^{\perp}\mathbf{L}\left(\mathbf{G}_a\mathbf{L}+\mathbf{W}\mathbf{W}^{\mathrm{T}}\right)^{-1}\mathbf{H} \tag{45}$$

The solution of Eq. (35) in whichever format is not the main concern of the present developments (Dumont, 2010b). This Section was devoted to establishing the conventional boundary element method in the most consistent way possible, as a means to further outline the core concepts of this paper.

Before doing that, however, one must outline as briefly as possible the main features of the simplified boundary element method, which is the subject of the next Section.

5 THE SIMPLIFIED HYBRID BOUNDARY ELEMENT METHOD

5.1 A brief introduction with reference to the hybrid boundary element method

The hybrid boundary element method (HBEM) was introduced about two decades ago on the basis of the Hellinger-Reissner potential, as a generalization of Pian's hybrid finite element method (Pian,1964; Dumont, 1987; Dumont, 1989). The formulation requires evaluation of integrals only along the boundary and makes use of fundamental solutions to interpolate fields in the domain. Accordingly, an elastic body of arbitrary shape may be treated as a single finite macro-element with as many boundary degrees of freedom as desired. The original method makes use of a flexibility matrix $\mathbf{F}^*$, for which evaluation of integrals along the entire boundary is required.

A simplified, although equally accurate, version of the HBEM was proposed about a decade ago (Dumont and Chaves, 2001). This simplified hybrid boundary element method (SHBEM) makes use of a displacement matrix that is obtained directly from the fundamental solution, with which the time-consuming evaluation of $\mathbf{F}^*$ is circumvented. In either formulation, submatrices about the main diagonal cannot be obtained by mathematical means: their evaluation requires the use of spectral properties related to either rigid-body displacements or simple displacement configurations.

This paper presents new theoretical developments that provide a solution that seems definitive and completely general. As outlined in Sections 5.3 and 5.5, the SHBEM relies basically on a virtual work statement and on a displacement compatibility equation. The key improvement has consisted in correctly applying a contragradient theorem, as in Section 5.6, to derive simple relations that are generally valid and can successfully substitute for the spectral properties that have been initially proposed. Actually, the hybrid virtual work principle of Section 5.3 had been identified since the onset of the SHBEM, but its application possibilities have not been visualized until recently. Now, once some simple stress or strain cases are identified as inherent to a given problem, it is always possible to find a set of linearly independent analytical solutions to provide sufficient equations for the evaluation of the still unknown coefficients, regardless of topology and spectral properties.

5.2 Stress and Displacement assumptions

Two independent trial fields are assumed, according to the hybrid methodology proposed by Pian. The displacement field is explicitly approximated along the boundary by u_i^d, exactly as proposed in Section 3.1, in the *external* reference system of the numerical problem. An independent stress field σ_{ij}^s, where $()^s$ stands for *stress assumption*, is given in the domain in terms of a series of fundamental solutions σ_{ijm}^* with global support, multiplied by point force parameters $\mathbf{p}^*$ applied at the same boundary nodal points m to which the nodal displacements d_m are attached, also exactly as proposed in Section 3.3 - this is the *internal* reference system of the numerical problem. Displacements u_i^s are obtained from σ_{ij}^s as in Eq. (17). Then, differently from the conventional boundary element method, one makes use of fundamental solutions as trial functions - not just weighting functions. Moreover, no assumptions are made on the traction-force behavior along Γ.

The Hellinger-Reissner potential, based on the two-field assumptions of the latter Section, as implemented by Pian (1964) and generalized by Dumont (1989), leads to two matrix equations that express nodal equilibrium and compatibility requirements. In the following simplified developments, the same equilibrium matrix equation is obtained in terms of virtual work (which is a

variational approach), but the set of compatibility equations is obtained by direct evaluation of displacements at the boundary nodal points (which is non-variational).

5.3 A displacement virtual-work statement

The equilibrium of forces acting on the elastic body, according to Eqs. (1) and (2), may be weakly enforced by

$$\int_\Omega \sigma_{ij}^s \delta u_{i,j}^d \,\mathrm{d}\Omega = \int_\Omega b_i \delta u_i^d \,\mathrm{d}\Omega + \int_{\Gamma_\sigma} \bar{t}_i \delta u_i^d \,\mathrm{d}\Gamma \tag{46}$$

since $\sigma_{ij}^s = \sigma_{ji}^s$. Integrating by parts the term at the left-hand side of Eq. (46), applying Green's theorem, and, finally, substituting for σ_{ij}^s and u_i^d according to Eqs. (11) and (5) (also observing that $\delta u_i^d = 0$ on Γ_u) leads to the expression

$$\delta d_n \left[\int_\Gamma \sigma_{ijm}^* \eta_j u_{in} \,\mathrm{d}\Gamma - \int_\Omega \sigma_{ijm,j}^* u_{in} \,\mathrm{d}\Omega \right] p_m^* = \delta d_n \left[\int_\Gamma t_i u_{in} \,\mathrm{d}\Gamma - \int_\Gamma \sigma_{ij}^p \eta_j u_{in} \,\mathrm{d}\Gamma \right] \tag{47}$$

Then, for arbitrary nodal displacements δd_n one obtains the matrix equilibrium equation

$$H_{mn} p_m^* = p_n - p_n^p \quad \text{or} \quad \mathbf{H}^{\mathrm{T}} \mathbf{p}^* = \mathbf{p} - \mathbf{p}^p \tag{48}$$

where $\mathbf{H}^{\mathrm{T}}$ is an equilibrium transformation matrix, the transpose of the same double-layer potential matrix that has already been introduced in the frame of the conventional boundary element method of Section 4. Recall that the domain integral of Eq. (47) is actually void, since σ_{ijm}^* are fundamental solutions and the domain Ω excludes the points of singularities of the point forces p_m^*. Moreover, $\mathbf{p} = [p_n] \in \mathbb{R}^{n^d}$ and $\mathbf{p}^p = [p_n^p] \in \mathbb{R}^{n^d}$, where

$$p_n = \int_\Gamma t_i u_{in} \,\mathrm{d}\Gamma \tag{49}$$

$$p_n^p = \int_\Gamma \sigma_{ji}^p \eta_j u_{in} \,\mathrm{d}\Gamma \tag{50}$$

are vectors of nodal forces that are equivalent, in terms of virtual work, to the applied traction t_i forces on the boundary and to the particular stress solution σ_{ij}^p for the domain forces b_i.

Equation (48) is fully consistent, as, according to the spectral properties of $\mathbf{H}$ already given in Eq. (39), only balanced equivalent forces $\mathbf{p} - \mathbf{p}^p$ can be transformed into a vector subset $\mathbf{p}^*$ that is related to a plain state of deformation, that is,

$$\mathbf{W}^{\mathrm{T}} (\mathbf{p} - \mathbf{p}^p) = \mathbf{0} \tag{51}$$

$$\mathbf{V}^{\mathrm{T}} \mathbf{p}^* = \mathbf{0} \tag{52}$$

In fact, for Neumann boundary conditions, Eq. (48), which is consistent because of Eq. (51) and (52), leads to a unique solution for $\mathbf{p}^*$ and thus via Eq. (11) to a unique stress state response in the domain.

It is worth noticing that, although Eq. (11) is valid for any p_m^*, a subset of $\mathbf{p}^*$ in the range of $\mathbf{V}$ shall yield a stress state that is void within discretization errors (Dumont-1989).

5.4 A contragradient expression of the displacement virtual-work statement

The *external* reference system $(\mathbf{d}, \mathbf{p})$, with nodal displacements $\mathbf{d}$ introduced in Eq. (5) and equivalent nodal forces $\mathbf{p}$ obtained in the frame of the virtual work statement that has led to Eq. (48), provides the numerical approximation of the actions along the boundary of the elastic body, rigid body displacements and unbalanced forces excluded. For mechanical consistency, the *internal*

reference system $(\mathbf{d}^*, \mathbf{p}^*)$ must approximate the corresponding domain stresses in terms of point forces $\mathbf{p}^*$, which perform work on equivalent nodal displacements $\mathbf{d}^*$, as defined in the following contragradient statement.

One starts with the virtual work statement

$$\delta\mathbf{p}^{*\mathrm{T}}\mathbf{P}_V^{\perp}\mathbf{d}^* = \delta\mathbf{p}^{\mathrm{T}}\mathbf{P}_W^{\perp}(\mathbf{d}-\mathbf{d}^p) \tag{53}$$

for virtual forces $\delta\mathbf{p}^*$ and $\delta\mathbf{p}$ that are in equilibrium, according to Eq. (48), and consistent with Eqs. (51) and (52). Substituting for $\delta\mathbf{p}$, one obtains, for arbitrary $\delta\mathbf{p}^*$,

$$\mathbf{H}\mathbf{P}_W^{\perp}(\mathbf{d}-\mathbf{d}^p) = \mathbf{P}_V^{\perp}\mathbf{d}^* \quad \text{or simply} \quad \mathbf{H}(\mathbf{d}-\mathbf{d}^p) = \mathbf{d}^* \tag{54}$$

as the orthogonal projectors $\mathbf{P}_W^{\perp}$ and $\mathbf{P}_V^{\perp}$ may be omitted with no harm to the consistency of the contragradient statement. This equation is integrant part of the variationally-based hybrid boundary element method and might be inferred to in the conventional boundary element method, as well, according to Eq. (33) (Dumont, 2003).

5.5 Nodal Displacement Compatibility

Application of the Hellinger-Reissner potential leads to, besides Eq. (46), a stress virtual work statement that enables writing a set of compatibility equations between nodal displacements $\mathbf{d}$ and equivalent nodal displacements $\mathbf{d}^*$ that are related to the *internal* reference system given in terms of fundamental solutions (Dumont and Chaves, 2001).[2]

Actually, one may dispense with any reference to the Hellinger-Reissner potential and simply establish that both eqs. (5) and (17) apply to the boundary nodal points, that is,

$$d_n - d_n^p = U_{nm}^* p_m^* + W_{ns} C_{sm} p_m^* \quad \text{or} \quad \mathbf{d}-\mathbf{d}^p = \mathbf{U}^*\mathbf{p}^* + \mathbf{W}\mathbf{C}\mathbf{p}^* \tag{55}$$

with the introduction of the nodal {\it displacement} matrix $\mathbf{U}^* = [U_{nm}^*] \in \mathbb{R}^{n^d \times n^d}$ and still in terms of a matrix $\mathbf{C}$ of rigid body displacements.

Let $\mathbf{U}_u^* = [U_{unm}^*] \in \mathbb{R}^{n^d \times n^d}$ be a block-diagonal matrix, with all coefficients equal to zero, except when m and n refer to the same nodal point, in which case U_{unm}^* is unknown. One may define a difference matrix $\mathbf{U}_e^* = \mathbf{U}^* - \mathbf{U}_u^*$ that has all its coefficients directly obtained in terms of the fundamental solution Eq. (55), that is, such that

$$\mathbf{U}^* = \mathbf{U}_e^* + \mathbf{U}_u^* \tag{56}$$

For singular fundamental solutions, the coefficients of $\mathbf{U}_u^*$ cannot be directly measured, as the singularity points are excluded from the domain Ω. This feature is consistent with the requirement

---

[2] This set of equations relies on the evaluation of a flexibility matrix $\mathbf{F}^* = [F_{mn}^*] \in \mathbb{R}^{n^d \times n^d}$, defined as $\int_\Gamma \sigma_{ijm}^* \eta_j u_{in}^* \mathrm{d}\Gamma$ (and that cannot be evaluated when m and n refer to the same nodal point), that enters in the equation $\mathbf{F}^*\mathbf{p}^* = \mathbf{H}\mathbf{d}$ that establishes compatibility in terms of equivalent nodal displacements and such that, for consistency, $\mathbf{F}^*\mathbf{V} = \mathbf{0}$, when dealing with a finite domain. Application of the formulation to the complementary unbounded domain $\overline{\Omega}$ leads to a flexibility matrix $\overline{\mathbf{F}}^*$ such that $\mathbf{F}^* + \overline{\mathbf{F}}^* = \mathbf{U}^*$, where $\mathbf{U}^* = [U_{nm}^*] \in \mathbb{R}^{n^d \times n^d}$ corresponds to the fundamental solution u_{im}^* measured as d_n at the nodal degree of freedom n for a unit point force p_m^* applied at the nodal degree of freedom m. However, no reference to the developments above are actually needed, as outlined in the following, in a framework that is computationally simpler, although no longer primarily related to a variational statement.

that u^*_{im} be analytical in Ω. Then, the coefficients of $\mathbf{U}^*_u$ can only be obtained by means of some global, problem-dependent, assessment of the linear algebra properties of Eq. (55) in conjunction with Eq. (48).

The reasoning of the above paragraph leads to the conclusion that, in a fully variational framework, but not as the direct outcome of a variational statement, one is entitled to transform point forces p^*_m into nodal displacements d_n by explicitly using the fundamental solution u^*_{im} as in Eq. (55). This has led to the *simplified* hybrid boundary element method, in which the time-consuming evaluation of the flexibility matrix $\mathbf{F}^*$ of the firstly developed, fully variational hybrid formulation could be circumvented.

Abstracting for the moment that $\mathbf{U}^*_u$ is still unknown, one may pre-multiply Eq. (55) by $\mathbf{W}^{\mathrm{T}}$ and solve for $\mathbf{C}\mathbf{p}^*$ in terms of the problem's primary parameters $\mathbf{d}$ and $\mathbf{p}^*$:

$$\mathbf{C}\mathbf{p}^* = \mathbf{W}^{\mathrm{T}}(\mathbf{d} - \mathbf{d}^p - \mathbf{U}^*\mathbf{p}^*) \tag{57}$$

Applied to Eq. (55), this expression leads to

$$\mathbf{P}^{\perp}_W \mathbf{U}^*\mathbf{p}^* = \mathbf{P}^{\perp}_W(\mathbf{d} - \mathbf{d}^p) \tag{58}$$

with introduction of the orthogonal projector $\mathbf{P}^{\perp}_W = \mathbf{I} - \mathbf{W}\mathbf{W}^{\mathrm{T}}$. Then, for a finite domain, only displacements that are orthogonal to rigid body motions can be transformed between the stress and displacement reference systems.

Assuming that $\mathbf{U}^*_u$ is known, it is possible to solve for $\mathbf{p}^*$ in Eqs. (48) and (58) and thus arrive at a matrix equation solely in terms of $\mathbf{d}$ and $\mathbf{p}$ - with the identification of a stiffness-type transformation matrix. However, $\mathbf{U}^*_0$ still has to be evaluated in a way that is both computationally feasible and mechanically sound.

5.6 A hybrid virtual work statement

As introduced in Sections 3.1 and 3.3, $\mathbf{d}$ and $\mathbf{p}^*$ are the primary unknowns of the problem, to which correspond equivalent nodal forces and displacements $\mathbf{p}$ and $\mathbf{d}^*$, respectively. The quantities $\mathbf{p}$ and $\mathbf{p}^*$ are interrelated by Eq. (48); $\mathbf{d}$ and $\mathbf{p}^*$ are interrelated by Eq. (59). At present, one is attempting to find an expression that interrelates the equivalent nodal quantities $\mathbf{p}$ and $\mathbf{d}^*$, for reasons that will be soon uncovered. Let a virtual stress state be represented by $\delta\mathbf{p}^*$ and $\delta\mathbf{d}$, as interrelated by Eq. (60). Only admissible subsets of $\delta\mathbf{p}^*$ and $\delta\mathbf{d}$ actually enter in Eq. (61), as the orthogonal projector $\mathbf{P}_W$ excludes the participation of any quantities related to rigid body displacements (or unbalanced forces). The virtual work $\delta\mathbb{W}(\mathbf{d})$ related to the conjugate $\left(\delta\mathbf{u}, \mathbf{P}^{\perp}_W(\mathbf{p} - \mathbf{p}^p)\right)$ and the complementary virtual work $\delta\mathbb{W}^C(\mathbf{p}^*)$ related to the conjugate $\left(\mathbf{P}^{\perp}_V\mathbf{d}^*, \delta\mathbf{p}^*\right)$ are given by

$$\delta\mathbb{W}(\mathbf{d}) = \delta\mathbf{d}^{\mathrm{T}}\mathbf{P}^{\perp}_W(\mathbf{p} - \mathbf{p}^p) \tag{62}$$

$$\delta\mathbb{W}^C(\mathbf{p}^*) = \delta\mathbf{p}^{*\mathrm{T}}\mathbf{P}^{\perp}_V\mathbf{d}^* \tag{63}$$

In the frame of the present linear elastic problem, $\delta\mathbb{W}(\mathbf{d})$ and $\delta\mathbb{W}^C(\mathbf{p}^*)$ are equivalent. Then, the following hybrid virtual work principle holds:

$$\delta\mathbf{d}^{\mathrm{T}}\mathbf{P}^{\perp}_W(\mathbf{p} - \mathbf{p}^p) = \delta\mathbf{p}^{*\mathrm{T}}\mathbf{P}^{\perp}_V\mathbf{d}^* \tag{64}$$

Substituting for $\delta\mathbf{u}^{\mathrm{T}}\mathbf{P}^{\perp}_W$ according to Eq. (65), one obtains

$$\delta\mathbf{p}^{*\mathrm{T}}\mathbf{U}^{*\mathrm{T}}\mathbf{P}_W^{\perp}(\mathbf{p}-\mathbf{p}^{p})=\delta\mathbf{p}^{*\mathrm{T}}\mathbf{P}_V^{\perp}\mathbf{d}^{*} \tag{66}$$

This expression is valid for any virtual set of point forces $\delta\mathbf{p}^{*}$ (not just the admissible ones). Thus,

$$\mathbf{U}^{*\mathrm{T}}\mathbf{P}_W^{\perp}(\mathbf{p}-\mathbf{p}^{p})=\mathbf{P}_V^{\perp}\mathbf{d}^{*} \tag{67}$$

This might be the final expression one is looking for. However, resorting to the contragradient Eq. (54), it is possible to arrive at a more convenient equation,

$$\mathbf{U}^{*\mathrm{T}}\mathbf{P}_W^{\perp}(\mathbf{p}-\mathbf{p}^{p})=\mathbf{H}(\mathbf{d}-\mathbf{d}^{p}) \tag{68}$$

that explicitly relates nodal displacements and equivalent nodal forces without the intervenience of the auxiliary set of forces $\mathbf{p}^{*}$, instead of the originally proposed double system of Eqs. (48) and (58) . The construction of a stiffness relation from Eq. (68) is not addressed in this paper (Oliveira, 2004).

5.7 Evaluation of the coefficients about the main diagonal of the matrix $\mathbf{U}^{*}$

Let $\mathbf{D}=[D_{ms}]\in\mathbb{R}^{n^d\times n^a}$ and $\mathbf{P}=[P_{ms}]\in\mathbb{R}^{n^d\times n^a}$ be two matrices whose columns are nodal displacements and equivalent nodal forces that correspond to a number n^a of simple analytical solutions (the superscript a stands for *analytical*). Equation (68) must pass a patch test, exactly as proposed by Zienkiewicz and Irons (Irons and Ahmad, 1970) in the frame of the displacement finite element method. Applying this solution to Eq. (68), one obtains

$$\mathbf{U}^{*\mathrm{T}}\mathbf{P}=\mathbf{H}\mathbf{U} \tag{69}$$

since $\mathbf{P}_W^{\perp}\mathbf{P}=\mathbf{0}$, or, for $\mathbf{U}^{*}$ split as in Eq. (56),

$$\mathbf{U}_u^{*\mathrm{T}}\mathbf{P}=\mathbf{H}\mathbf{U}-\mathbf{U}_e^{*\mathrm{T}}\mathbf{P} \tag{70}$$

For potential problems, $\mathbf{U}_u^{*}$ is a diagonal matrix. There are $n^a=2$ and $n^a=3$ simple analytical solutions for 2D and 3D potential problems, respectively, as potentials that vary linearly in the coordinate directions. For elasticity problems, the non-zero values of $\mathbf{U}_u^{*}$ comprise a block-diagonal matrix with 2×2 and 3×3 submatrices for 2D and 3D problems, respectively. There are $n^a=3$ and $n^a=6$ simple analytical solutions for 2D and 3D elasticity problems, respectively, for displacements that vary linearly in the coordinate directions, rigid body rotations excluded. These solutions are presented in Appendix A in a more general framework. Then, there are more analytical, linear solutions available than unknowns for each row of uncoupled equations represented by Eq. (70). The best procedure is to solve for each row in terms of least squares, which means that no direction is preferred in the solution and, most important, making sure that the resultant matrix of the equation system is always well conditioned regardless of spatial orientation of the boundary segments that are adjacent to each nodal point (since the orientation of the boundary normal vectors enters in the evaluation of the equivalent nodal forces $\mathbf{P}$.

It is worth noticing that, for elasticity problems, each row of unknowns of $\mathbf{U}_u^{*}$ in Eq. (70) is best solved separately from the remaining rows related to the same node, as there is no mechanical basis to enforce that the block-diagonal matrices of $\mathbf{U}_u^{*}$ be symmetric, although $\mathbf{U}_e^{*}$ is symmetric by construction - the origin of $\mathbf{U}^{*}$ in Eq. (55) is not directly related to a variational statement. In fact, as tested by Oliveira (2004), numerical results obtained using a coarse mesh do not improve by enforcing symmetry of $\mathbf{U}_u^{*}$, although $\mathbf{U}_u^{*}$ tends to become symmetric with mesh refinement. Observe also that, owing to the fact that $\mathbf{P}_W^{\perp}\mathbf{P}=\mathbf{0}$ and $\mathbf{H}\mathbf{W}=\mathbf{0}$, no rigid body displacements interfere with Eq. (69).

5.8 Comparison of the conventional and the simplified hybrid boundary element methods

Equation (68) may be rewritten by substituting for the equivalent nodal forces according to Eq. (20),

$$\mathbf{H}(\mathbf{d}-\mathbf{d}^{p})=\mathbf{U}^{*\mathrm{T}}\mathbf{P}_{W}^{\perp}\mathbf{L}^{\mathrm{T}}(\mathbf{t}-\mathbf{t}^{p}) \tag{71}$$

and compared with Eq. (35), obtained in the frame of the conventional, however consistent, collocation boundary element method, reproduced below:

$$\mathbf{H}\left(\mathbf{d}-\mathbf{d}^{p}\right)=\mathbf{G}\mathbf{P}_{Z}^{\perp}\left(\mathbf{t}-\mathbf{t}^{p}\right) \tag{72}$$

Then, the simplified hybrid boundary element method has led with Eq. (71) to an expedite expression of the consistent single-layer matrix $\mathbf{G}\mathbf{P}_{Z}^{\perp}$ of the conventional boundary element method, which is in general computationally expensive to be accurately evaluated owing to the improper integral term that has to be resolved. The evaluation of the corresponding matrix in Eq. (71) only requires the evaluation of the banded matrix $\mathbf{L}$ (which can be stored as a sparse matrix) and of the few columns of equivalent nodal forces of the matrix $\mathbf{P}$ in Eq. (69), with all integrations carried out in terms of a Gauss-Legendre quadrature. The least-square solution of the series of small uncoupled systems of equations in Eq. (70) is rather inexpensive. One observes that, in general, the matrices on the right-hand side of Eqs. (71) and (72) are different from each other, particularly in terms of null spaces:

$$N\left(\mathbf{U}^{*\mathrm{T}}\mathbf{P}_{W}^{\perp}\mathbf{L}^{\mathrm{T}}\right)\neq N\left(\mathbf{G}\mathbf{P}_{Z}^{\perp}\right) \tag{73}$$

However, it is expected that, if the numerical models represented by Eqs. (71) and (72)converge to the idealized mechanical problem with increasing mesh refinement, then it is possible to have a boundary mesh refined in such a way that

$$\|\,\mathbf{U}^{*\mathrm{T}}\mathbf{P}_{W}^{\perp}\mathbf{L}^{\mathrm{T}}-\mathbf{G}\mathbf{P}_{Z}^{\perp}\,\|\leq\epsilon \tag{74}$$

for an arbitrarily small error ϵ and any given norm $\|\bullet\|$.

It is remarkable how two basically different methods - the conventional boundary element method and the simplified-hybrid boundary element method - seemingly converge to the same final equations. Nevertheless, the developments of this Section - in terms of virtual work statements, contragradient assumptions (or theorems) and a patch test - may be further extended in the direction of a more simplified, expedite, formulation of the boundary element method, as shown in the next Section.

The next Section compares concepts of both methods for the evaluation of results at internal points and a numerical example is presented.

6 AN EXPEDITE FORMULATION OF THE BOUNDARY ELEMENT METHOD

Equation (55) has a variational justification - the hybrid boundary element method applied to a finite domain and then to its complementary, unbounded domain[Reference????]. However, this equation was introduced as just a plausible assumption that becomes validated both in terms of linear algebra consistency of the resultant matrix equations and numerically. One goes one step further and assumes that, if Eq. (55) is valid, then one also may evaluate boundary traction forces, according to Eq. (2) for the entire boundary Γ, directly from the fundamental solutions of Eq. (11) as

$$\mathbf{t}-\mathbf{t}^{p}=\mathbf{T}^{*}\mathbf{p}^{*} \tag{75}$$

where $\mathbf{T}^{*}=[T^{*}_{mn}]\in\mathbb{R}^{n^{t}\times n^{d}}$ is a generally rectangular matrix. This matrix transforms the point force parameters $\mathbf{p}^{*}$ of the series of fundamental solutions of the internal reference system into traction

forces $\mathbf{t}$ measured at the extremities of the boundary segments adjacent to the nodal points, according to the definition of the traction-force parameters of Eq. (10).

As proceeded in Section 5.7 for dealing with the displacement matrix $\mathbf{U}^*$, let $\mathbf{T}_u^* = [T_{u\,mn}^*] \in \mathbb{R}^{n^t \times n^d}$ be a block-diagonal matrix, with all coefficients equal to zero, except when m and n refer to the same nodal point, in which case $T_{u\,mn}^*$ is unknown. One may define a difference matrix $\mathbf{T}_e^* = \mathbf{T}^* - \mathbf{T}_u^*$ that has all its coefficients directly obtained in terms of the fundamental solution Eq. (11), that is, such that

$$\mathbf{T}^* = \mathbf{T}_e^* + \mathbf{T}_u^* \tag{76}$$

For singular fundamental solutions, the coefficients of $\mathbf{T}_u^*$ cannot be directly measured, as the singularity points are excluded from the domain Ω. This feature is consistent with the requirement that σ_{ijm}^* be analytical in Ω. Then, the coefficients of $\mathbf{T}_u^*$ can only be obtained by means of some global, problem-dependent, assessment of the linear algebra properties of $\mathbf{T}^*$ in eq. (75) in conjunction with other matrix relations, some of them are still to be introduced.

In terms of a variational analysis, $\mathbf{t}$ are Lagrangian multipliers that perform virtual work on equivalent nodal displacements that are here defined as $\mathbf{d}^t$ (and may be rather difficult to understand physically). The conjugate quantities $(\mathbf{t}, \mathbf{d}^t)$ represent an auxiliary reference system for the deformation state of the elastic body, for numerical discretization schemes as proposed in Section 3. Then, one may write the following virtual work statement, for virtual forces $\delta\mathbf{t}$ and $\delta\mathbf{p}$ that are in equilibrium:

$$\delta\mathbf{p}^{\mathrm{T}}\mathbf{P}_W^{\perp}(\mathbf{d}-\mathbf{d}^p) = \delta\mathbf{t}^{\mathrm{T}}\mathbf{P}_Z^{\perp}(\mathbf{d}^t-\mathbf{d}^{tp}) \tag{77}$$

This procedure is in accordance with the ones of Sections 5.4 and 5.6, for a deformed state represented in terms of nodal displacements $\mathbf{P}_W^{\perp}(\mathbf{d}-\mathbf{d}^p)$ of the external reference system, which are compatible with equivalent displacements $\mathbf{P}_Z^{\perp}(\mathbf{d}^t-\mathbf{d}^{tp})$ of the auxiliary system (where $\mathbf{d}^{tp}$ is formally defined as equivalent to the domain forces b_i). Substituting for $\delta\mathbf{p}$ from Eq. (20), one obtains, for arbitrary $\delta\mathbf{t}$,

$$\mathbf{L}\mathbf{P}_W^{\perp}(\mathbf{d}-\mathbf{d}^p) = \mathbf{P}_Z^{\perp}(\mathbf{d}^t-\mathbf{d}^{tp}) \tag{78}$$

On the other hand, it is also possible to relate the equivalent displacements $\mathbf{P}_Z^{\perp}(\mathbf{d}^t-\mathbf{d}^{tp})$ of the auxiliary system to the equivalent nodal displacements $\mathbf{P}_V^{\perp}\mathbf{d}^*$ of the internal reference system, for and admissible deformed state, in terms of the virtual work performed by forces $\delta\mathbf{t}$ and $\delta\mathbf{p}^*$ that are in equilibrium:

$$\delta\mathbf{p}^{*\mathrm{T}}\mathbf{P}_V^{\perp}\mathbf{d}^* = \delta\mathbf{t}^{\mathrm{T}}\mathbf{P}_Z^{\perp}(\mathbf{d}^t-\mathbf{d}^{tp}) \tag{79}$$

Substituting for $\delta\mathbf{t}$ from Eq. (75), one obtains, for arbitrary $\delta\mathbf{p}^*$,

$$\mathbf{P}_V^{\perp}\mathbf{d}^* = \mathbf{T}^{*\mathrm{T}}\mathbf{P}_Z^{\perp}(\mathbf{d}^t-\mathbf{d}^{tp}) \tag{80}$$

Finally, one substitutes in this equation for $\mathbf{P}_V^{\perp}\mathbf{d}^*$ according to Eq. (54), and for $\mathbf{P}_Z^{\perp}(\mathbf{d}^t-\mathbf{d}^{tp})$ according to Eq. (78), thus arriving at

$$\mathbf{H}(\mathbf{d}-\mathbf{d}^p) = \mathbf{T}^{*\mathrm{T}}\mathbf{L}\mathbf{P}_W^{\perp}(\mathbf{d}-\mathbf{d}^p) \tag{81}$$

Since this equation must be valid for any nodal displacements (rigid body displacements included), $\mathbf{T}^{*\mathrm{T}}\mathbf{L}\mathbf{P}_W^{\perp}$ is an approximation of $\mathbf{H}$, provided that the still unknown coefficients of $\mathbf{T}_u^*$ are evaluated. One observes that, by construction, $N(\mathbf{T}^{*\mathrm{T}}\mathbf{L}\mathbf{P}_W^{\perp}) = N(\mathbf{H})$. In principle, a simple

means to evaluate $\mathbf{T}_u^*$ would be by imposing that $N(\mathbf{P}_W^{\perp}\mathbf{L}^{\mathrm{T}}\mathbf{T}^*) = N(\mathbf{H}^{\mathrm{T}})$, which would lead to full consistency of Eq. (71). However, as already mentioned in Footnote 2, one can rely on the coefficients of $\mathbf{V}$ only for strictly convex domains[3].

The best procedure seems to follow the scheme proposed in Section 5.7 and evaluate $\mathbf{T}_u^*$ in Eq. (81) in the frame of a patch test for a set of simple analytical solutions of the problem. If the numerical models represented by Eq. (72) and by using the approximate matrix of Eq. (81) converge to the idealized mechanical problem with increasing mesh refinement, then it is possible to have a boundary mesh refined in such a way that

$$\| \mathbf{T}^{*\mathrm{T}}\mathbf{L}\mathbf{P}_W^{\perp} - \mathbf{H} \| \leq \epsilon \tag{82}$$

for an arbitrarily small error ϵ and any given norm $\| \bullet \|$.

Before proposing a scheme for the evaluation of $\mathbf{T}_u^*$, one is encouraged to move on in the present developments by comparing Eqs. (68) and (81), thus writing

$$\mathbf{T}^{*\mathrm{T}}\mathbf{L}\mathbf{P}_W^{\perp}(\mathbf{d} - \mathbf{d}^p) = \mathbf{U}^{*\mathrm{T}}\mathbf{P}_W^{\perp}(\mathbf{p} - \mathbf{p}^p) \tag{83}$$

or, else, making use of Eq. (20) and according to Eq. (71),

$$\mathbf{T}^{*\mathrm{T}}\mathbf{L}\mathbf{P}_W^{\perp}(\mathbf{d} - \mathbf{d}^p) = \mathbf{U}^{*\mathrm{T}}\mathbf{P}_W^{\perp}\mathbf{L}^{\mathrm{T}}(\mathbf{t} - \mathbf{t}^p) \tag{84}$$

This equation may be compared with Eq. (35) from the conventional boundary element method, here repeated once more:

$$\mathbf{H}\left(\mathbf{d} - \mathbf{d}^p\right) = \mathbf{G}\mathbf{P}_Z^{\perp}\left(\mathbf{t} - \mathbf{t}^p\right) \tag{85}$$

One concludes that Eqs. (83) and (84) are expedite ways of constructing an equation system that circumvents the need of carrying out any singular or quasi-singular integral and in fact requires the Gauss-Legendre integration of relatively few coefficients. The application possibilities of the equations above to solve a numerical problem is discussed in Section 7.

It is worth extending the scheme proposed in Section 5.7 and suggesting a means for the evaluation of the unknown terms of both $\mathbf{U}_u^*$ and $\mathbf{T}_u^*$ in one and the same numerical framework. One may apply Eq. (83) to a set of deformed states corresponding to a sufficient number n^a of simple analytical solutions, by making use of the split expressions of Eqs. (56) and (76), with the unknowns written formally on the left-hand side:

$$\mathbf{T}_u^{*\mathrm{T}}\mathbf{L}\mathbf{P}_W^{\perp}\mathbf{D} - \mathbf{U}_u^{*\mathrm{T}}\mathbf{P} = -\mathbf{T}_e^{*\mathrm{T}}\mathbf{L}\mathbf{P}_W^{\perp}\mathbf{D} + \mathbf{U}_e^{*\mathrm{T}}\mathbf{P} \tag{86}$$

The number of unknown coefficients of $\mathbf{U}_u^*$ per row of the resulting uncoupled systems of equations derived from equation above is already discussed in the paragraph the follows Eq. (70). For a nodal point on a smooth boundary, the unknown coefficients of $\mathbf{T}_u^*$ are equal to 1, 2 or 3 for potential, 2D or 3D elasticity problems, respectively. Then, the total number of unknowns for $\mathbf{U}_u^*$ and $\mathbf{T}_u^*$ per row are respectively 2, 4 or 6, and a sufficient number n^a of simple analytical solutions may be envisaged to construct a system of equations that solves for $\mathbf{U}_u^*$ and $\mathbf{T}_u^*$ in a least-squares sense.

7 NUMERICAL EXAMPLES

Figure 2 shows two irregularly shaped domains for which the equations and concepts outlined in

[3] The spectral property just outlined is not sufficient to solve the problem, as $\mathbf{P}_W^{\perp}\mathbf{L}^{\mathrm{T}}\mathbf{T}^*$ is already by construction singular. This is related to the impossible task of finding $\mathbf{U}_u^*$ from Eq. (68) by imposing that $\mathbf{P}_W^{\perp}\mathbf{U}^*\mathbf{V} = \mathbf{0}$.

this paper shall be tested numerically in the frame of the solution of the 2D Laplace equation. One illustrates on the left an irregularly-shaped continuum for a set of five numerical examples, which present the same conceptual issues as in an elasticity problem. The mesh shown corresponds to examples M2_quad and M2_quadN, with a total of 62 quadratic elements and 124 nodes (46 elements along the external boundary and 16 elements modeling the hole indicated). There are also examples M1_quad and M1_quadN, with the same shapes of examples M2_quad and M2_quadN, but with 23 quadratic elements and 46 nodes only along the external boundary (no hole is modeled), as well as example M1_lin with the same mesh as before, but comprising 46 linear elements. In the examples M2_quad and M1_quad, polynomials $t_{i\ell}$ are used to build up the matrices $\mathbf{G}$ and $\mathbf{L}$. In the examples M2_quadN and M1_quadN, on the other hand, $t_{i\ell}$ is defined according to eqn (10). One is dealing with a non-convex domain, with a pronounced notch (whose tip is node 17 for the finer mesh and 9 for the coarse one) and a hole, in case of the finer mesh, comprised by nodes numbered 93 through 124.

On the right, Figure 2 illustrates a quadrilateral continuum made of five cubic elements, with a total of 15 nodes, whose corner coordinates are (0, 0), (15, 0), (10, 12) and (0, 12). One of the straight edges has a finer mesh, which results in elements of disparate sizes that may lead to some accuracy loss of the numerical model. The code implementation was in Maple language using 15 digits precision.

Since one did not want to worry about numerical integration issues, eight points were used in the Gauss-Legendre quadratures as well as in the quadratures with logarithmic weights, for integrations carried out along each boundary segment between two consecutive nodes. A far smaller number of integration points would be required - and far better accuracy achieved - if one had employed the numerical techniques preconized by Dumont and Noronha (1998).

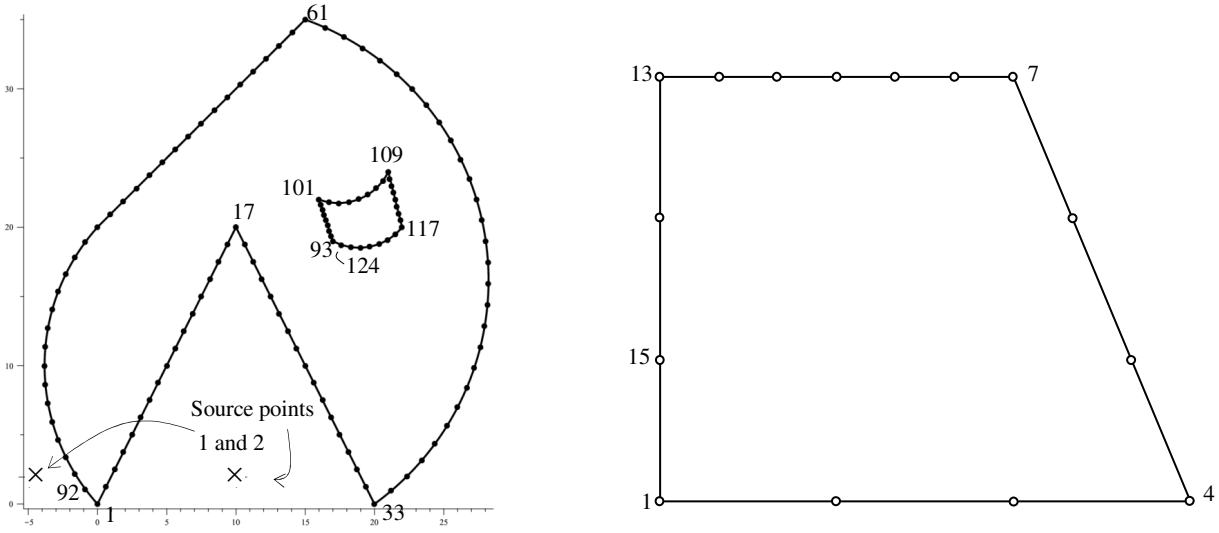

Figure 2: Discretization schemes to illustrate six numerical examples.

The primary accuracy check, as shown in the first row of Table 1, concerns the fact that one should have $\mathbf{HW} = \mathbf{0}$, according to Eq. (39). A relative error in terms of the Euclidian norm of matrices was established, as follows for the matrix product $\mathbf{HW}$, but similarly used in the subsequent rows:

$$|\mathbf{HW}| = \sqrt{\sum_m \left(\sum_n H_{mn} W_n \right)^2} \Big/ \sqrt{\sum_m \left(\sum_n |H_{mn} W_n| \right)^2} \tag{87}$$

$$\max |\mathbf{HW}| = \max \sqrt{\left(\sum_n H_{mn} W_n \right)^2} \Big/ \sqrt{\left(\sum_n |H_{mn} W_n| \right)^2} \tag{88}$$

The larger errors in the last columns of Table 1 are mainly due to quasi-singularity issues related to the elements around corner points and particularly around the notch tip, which could have been avoided, if strictly necessary (Dumont and Noronha, 1998). The errors indicated in the first row are given as just an estimate of the maximal accuracy one should expect in the subsequent rows of results. The second row indicates that the null space of $\mathbf{V} = N\left(\mathbf{H}^{\mathrm{T}}\right)$, introduced in Eq. (40), could be evaluated very accurately. One obtains in the third row that the stiffness-like matrix of Eq. (44), although spectrally inconsistent by construction, actually leads to forces that are almost in balance. In the fourth row, one evaluates the errors related to the expedite matrix $\mathbf{U}^{*\mathrm{T}}\mathbf{L}^{\mathrm{T}}$ that substitutes for the single layer potential matrix $\mathbf{G}$ (in the error norms, obtained similarly to Eqs. (87) and (88), the Euclidian norm of $\mathbf{G}$ is used in the denominators). The fifth row shows that the admissible matrix $\mathbf{G}_a$ is almost orthogonal to $N\left(\mathbf{H}^{\mathrm{T}}\right)$, as one should expect. The same happens with its consistent substitute $\mathbf{U}^{*\mathrm{T}}\mathbf{P}_W^{\perp}\mathbf{L}^{\mathrm{T}}$, as shown in the sixth row, except for the coarse mesh of cubic elements. The seventh row deals with the substitute $\mathbf{T}^{*\mathrm{T}}\mathbf{L}$ of the second layer potential matrix $\mathbf{H}$, in the same way as explained for the fifth row, although showing larger relative errors (which is conceptually explainable). The last row displays the errors of $\mathbf{T}^{*\mathrm{T}}\mathbf{L}$ in terms of its orthogonality to $N\left(\mathbf{H}^{\mathrm{T}}\right)$, with reasonable results even for the coarsest mesh.

	M1_lin	M1_quad	M1_quadN	M2_quad	M2_quadN	M3_cub
$\lvert\mathbf{HW}\rvert$	.239e-10	.223e-10	.223e-10	.565e-7	.565e-7	.222e-7
$\max\lvert\mathbf{HW}\rvert$	.725e-10	.725e-10	.725e-10	.400e-6	.400e-6	.730e-7
$\lvert\mathbf{H}^{\mathrm{T}}\mathbf{V}\rvert$	.366e-11	.362e-11	.362e-11	.246e-12	.246e-12	.218e-8
$\max\lvert\mathbf{H}^{\mathrm{T}}\mathbf{V}\rvert$	.108e-10	.170e-10	.170e-10	.242e-11	.242e-11	.617e-8
$\lvert\mathbf{K}^{\mathrm{T}}\mathbf{W}\rvert$	.688e-3	.167e-2	.168e-2	.798e-3	.799e-3	.311e-2
$\max\lvert\mathbf{K}^{\mathrm{T}}\mathbf{W}\rvert$	.499e-2	.295e-2	.297e-2	.166e-2	.166e-2	.899e-2
$\lvert\mathbf{U}^{*\mathrm{T}}\mathbf{L}^{\mathrm{T}}-\mathbf{G}\rvert$	.151e-1	.946e-2	.950e-2	.589e-2	.590e-2	.324e-1
$\max\lvert\mathbf{U}^{*\mathrm{T}}\mathbf{L}^{\mathrm{T}}-\mathbf{G}\rvert$	.671e-1	.920e-1	.925e-1	.460e-1	.461e-1	.175
$\lvert\mathbf{G}_a^{\mathrm{T}}\mathbf{V}\rvert$	.545e-2	.442e-2	.448e-2	.232e-2	.233e-2	.105e-1
$\lvert\mathbf{L}\mathbf{P}_W^{\perp}\mathbf{U}^{*}\mathbf{V}\rvert$	.158e-2	.522e-3	.523e-3	.243e-3	.243e-3	.848e-2
$\lvert\mathbf{T}^{*\mathrm{T}}\mathbf{L}-\mathbf{H}\rvert$	.132e-1	.810e-2	.809e-2	.166e-1	.166e-1	.202e-1
$\max\lvert\mathbf{T}^{*\mathrm{T}}\mathbf{L}-\mathbf{H}\rvert$	.120e-1	.118e-1	.118e-1	.533e-1	.533e-1	.190e-1
$\lvert\mathbf{L}^{\mathrm{T}}\mathbf{T}^{*}\mathbf{V}\rvert$	.488e-2	.324e-2	.324e-2	.255e-2	.255e-2	.548e-2

Table 1: Euclidean norms of several matrix products.

One also runs a series of patch tests for a total of ten potential fields applied to the models. Eight of them, numbered 1 to 8, are listed as the following four pairs, $\left\langle x \quad y \quad xy \quad x^2-y^2 \quad x^3-3xy^2 \quad -3x^2y+y^3 \quad x^4+y^4-6x^2y^2 \quad x^3y-xy^3 \right\rangle$, corresponding to linear, quadratic, cubic and quartic fields. The potential fields numbered 9 and 10 correspond to $\ln(r)/2\pi$, where r is the distance to the source points (-5, 2) and (10, 2) marked as two crosses on the left of Figure 2. For the coarse mesh with cubic elements, the source points are (-5, 2) and (5,

15). The accuracy of the solutions in the frame of the conventional, collocation boundary element method - with the inconsistent matrix $\mathbf{G}$ in Eq. (33) - is assessed in the first graphic of Figure 3, for all ten potential fields, with corresponding values of $\mathbf{d}$ and $\mathbf{t}$ evaluated analytically (the results using $\mathbf{G}_a$, as in Eq. (35), are almost indistinguishable from the ones with $\mathbf{G}$).

The second graphic in Figure 3 assesses the accuracy of using $\mathbf{L}^{\mathrm{T}}$, as given in Eq. (21), to evaluate equivalent nodal gradients, for $\mathbf{p}$ directly integrated as $p_m = \int_\Gamma u_{im} t_i \mathrm{d}\Gamma$. The last graphic assesses the accuracy of the 'stiffness' system of Eq. (43), where $\mathbf{K}$ is the inconsistent matrix of Eq. (44). Numerical results using alternative definitions of $\mathbf{K}$ are almost indistinguishable from these ones.

The curved parts of the boundaries are very deleterious to the numerical accuracy, particularly affecting the error norm $\left|\mathbf{L}^{\mathrm{T}}\mathbf{t}-\mathbf{p}\right|$. One checks that the use of $t_{i\ell}$ according to Eq. (10) significantly improves the problems' response to constant gradients, in terms of both $\left|\mathbf{L}^{\mathrm{T}}\mathbf{t}-\mathbf{p}\right|$ and $\left|\mathbf{H}\mathbf{d}-\mathbf{G}\mathbf{t}\right|$, but does not lead to perceptible improvements when testing for higher order gradients. However, the simplification achieved with Eq. (10) regarding numerical implementation is per se an improvement. Owing to the errors introduced by the approximation $\mathbf{p} \approx \mathbf{L}^{\mathrm{T}}\mathbf{t}$ for curved boundaries, results in terms of $\left|\mathbf{H}\mathbf{d}-\mathbf{G}\mathbf{t}\right|$ are in general significantly better than in terms of $\left|\mathbf{K}\mathbf{d}-\mathbf{p}\right|$.

In the first two graphics of Figure 4, the *unevaluated* coefficients of $\mathbf{U}^*$ and $\mathbf{T}^{*\mathrm{T}}\mathbf{L}$ are obtained through the comparison with results using the matrix $\mathbf{H}$, for constant gradients, as given by Eqs. (70) and (81), and then error estimates are given for the applied potential fields. In the third graphic, the results using $\mathbf{U}^*$ and $\mathbf{T}^{*\mathrm{T}}\mathbf{L}$, evaluated as mentioned above, are confronted. Finally, Figure 5 presents results for the *unevaluated* coefficients of $\mathbf{U}^*$ and $\mathbf{T}^{*\mathrm{T}}\mathbf{L}$ obtained without any reference to the matrix $\mathbf{H}$, but rather by simply imposing that $\left|\mathbf{T}^{*\mathrm{T}}\mathbf{L}\mathbf{D}-\mathbf{T}^{*\mathrm{T}}\mathbf{P}\right| = \min$ for a sufficient number of simple potential fields characterized by the conjugate sets $(\mathbf{D},\mathbf{P})$ of potentials and equivalent gradients. The results enable to conclude that, at least for the most refined mesh and despite curved boundaries, accuracy of about three digits is achieved. One observes that, in the outlined expedite formulation, the use of $t_{i\ell}$ as either polynomials or according to Eq. (10) turns out to be irrelevant as concerning accuracy, although Eq. (10) leads to simpler code writing and less computational time in the evaluation of $\mathbf{L}$.

8 CONCLUSIONS

The present developments are an attempt to arrive at a boundary element formulation that is as simple as possible and that also requires almost no numerical integrations. The Eqs. (83) and (84) are straightforward and effortless to implement and evaluate. They are also the seed of some new developments that may at least match the efficiency of the current fast multipole methods. Owing to space restrictions, this paper had to be devoted to the outline of the most fundamental concepts and to demonstrate - by means of some simple examples - the feasibility of numerically implementing such concepts. A second paper is being prepared to outline, as user friendly as possible, the basic features of the method as well as the algorithm that leads to the evaluation of $\mathbf{U}_u^*$ and $\mathbf{T}_u^{*\mathrm{T}}\mathbf{L}$ in either Eq. (83) or (84). Focus will also be given to the direct evaluation of results at internal points, for which no boundary integrations are required. Work is in progress to implement the expedite boundary element method for large scale, time-dependent, 2D and 3D problems.

9 ACKNOWLEDGMENTS

This research work was supported by the Brazilian agencies CAPES, CNPq and FAPERJ.

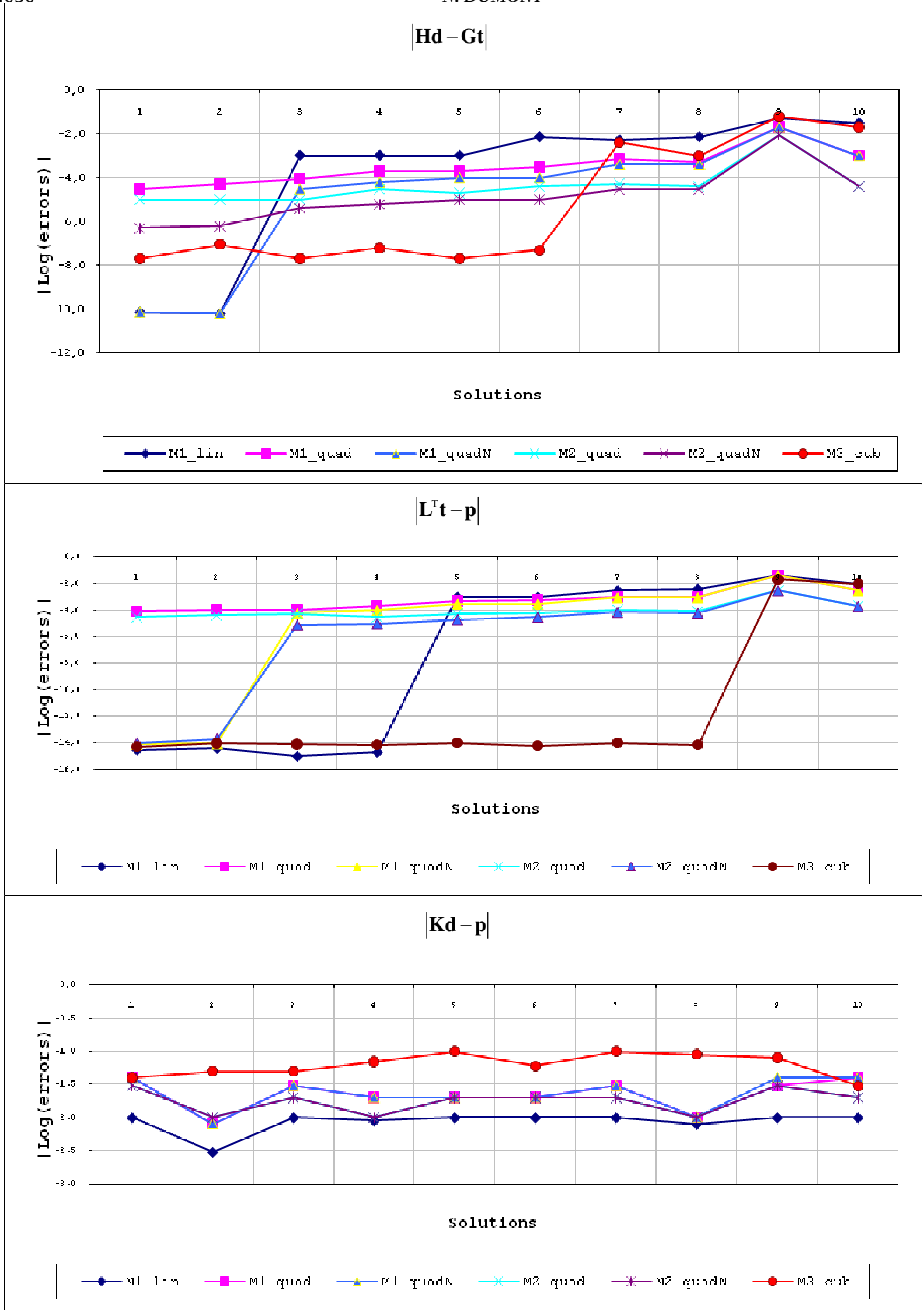

Figure 3: Error norms for three matrix equations from the collocation boundary element method.

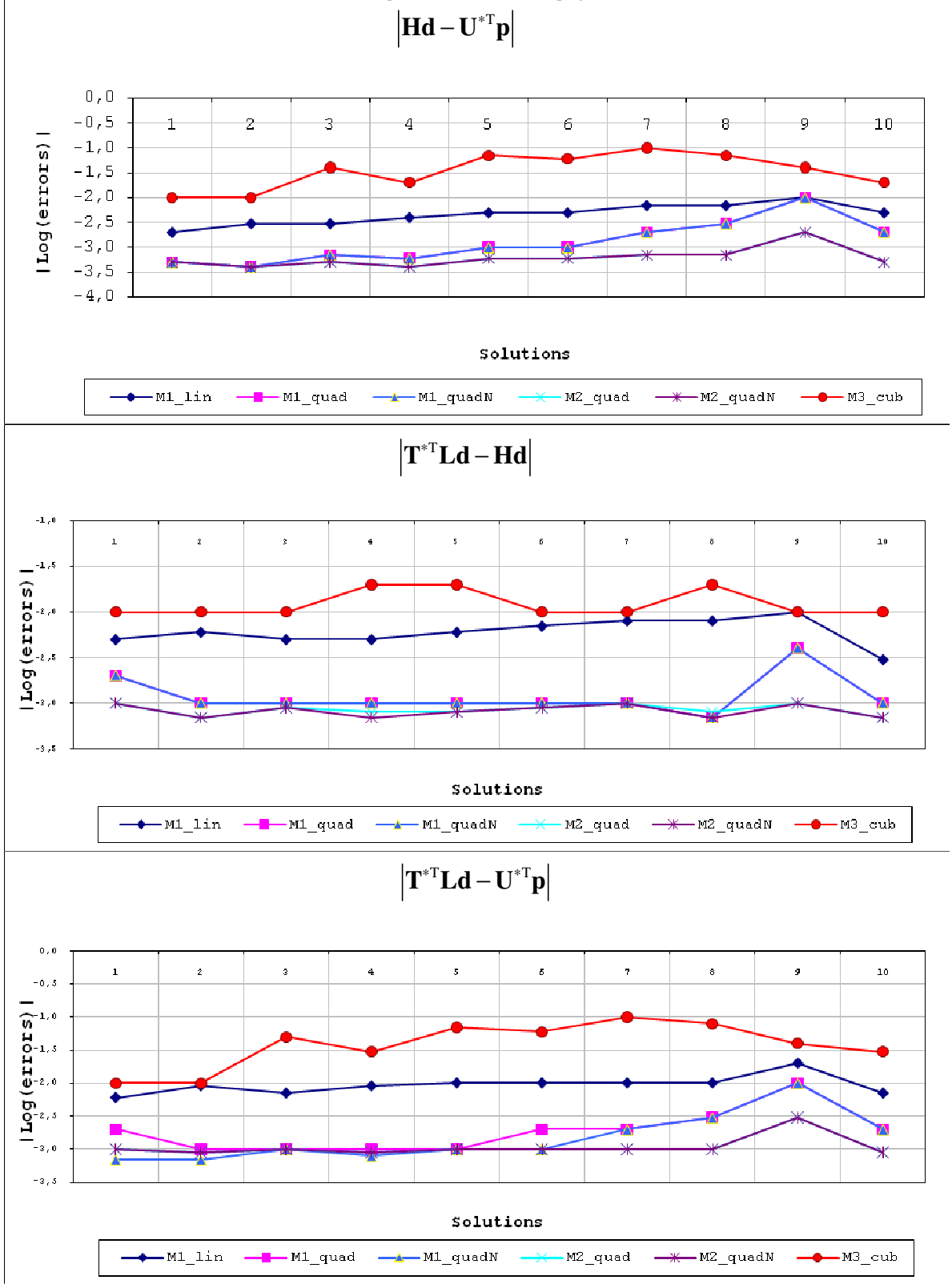

Figure 4: Error norms for the expedite boundary element methods.

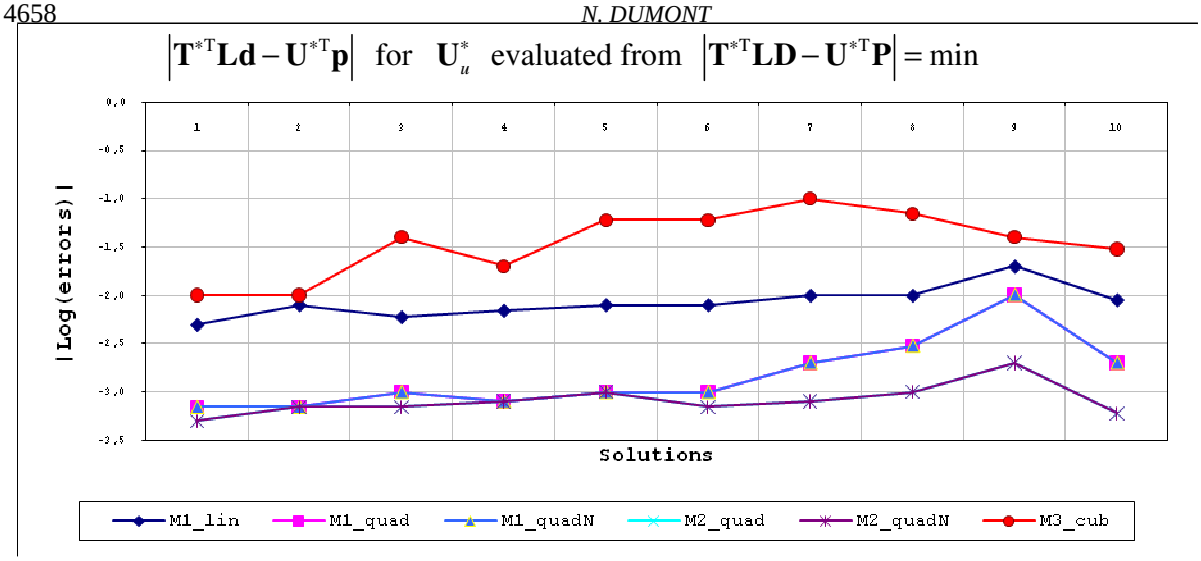

Figure 5: Error norms for the ultimate formulation of the expedite boundary element method.

REFERENCES

Ben-Israel, A, and Greville, T.N.E., *Generalized Inverses: Theory and Applications* (2nd edn). Springer-Verlag, 2003.

Brebbia, C.A., Telles, J.C.F., and Wrobel, L.C., *Boundary Element Techniques*, Springer-Verlag, 1984.

Dumont, N.A., The hybrid boundary element method. In *Boundary Elements IX, Vol 1: Mathematical and Computational Aspects*, eds. Brebbia, C.A., Wendland W. and Kuhn G., Computational Mechanics Publications, Springer-Verlag, 125-138,1987.

Dumont, N.A., and Chaves R.A.P., Simplified hybrid boundary element method applied to general time-dependent problems. In *Computational Mechanics - New Frontiers for the New Millenium - Proceedings of the First Asian-Pacific Congress on Computational Mechanics*, Sydney, Australia, eds. Valliappan S, Khalili N, Elsevier Science Ltd, 1009-1018, 2001.

Dumont, N.A., and Oliveira, M.F.F., and Chaves, R.A.P., Conventional, hybrid and simplified boundary element methods. In *Boundary Elements XXVI*, ed. Brebbia C.A., WIT-Press, 23-33, 2004.

Dumont N.A., and Oliveira, R., From frequency-dependent mass and stiffness matrices to the dynamic response of elastic systems. *Int J of Solids and Structures* 38(10-13):1813-1830, 2001.

Dumont N.A., and Oliveira, R., Fundamentals of the hybrid displacement boundary element method. In *Boundary Elements XXII*, eds. Brebbia CA, Power H, WIT Press, 145-154, 2000.

Dumont, N.A., and Noronha, M.A.M., A Simple, Accurate Scheme for the Numerical Evaluation of Integrals with Complex Singularity Poles. *Computational Mechanics* 22(1):42-49, 1998.

Dumont, N.A., and Alves, M.C., Symmetric and Antisymmetric Problems in the Hybrid Boundary Element Method. *Third Joint Conference of Italian Group of Computational Mechanics and Ibero-Latin American Association of Computational Methods in Engineering*, Giulianova, Italy, 10 pp on CD, 2002.

Dumont, N.A., and Chaves, R.A.P., and Paulino, G.H., The Hybrid Boundary Element Method Applied to Problems of Potential of Functionally Graded Materials. *International Journal of Computational Engineering Science* (IJCES), 5(4):863-891, 2004.

Dumont, N.A., and Huaman, D., A family of 2D and 3D hybrid finite elements for strain gradient elasticity. In *Advances in Boundary Element Techniques XI, Proceedings of the 11th International Conference*, eds. C. Zhang, M. H. Aliabadi, M. Schanz, Berlin, Germany, 144-153, 2010.

Dumont, N.A., and Lopes, A.A.O., On the Explicit Evaluation of Stress Intensity Factors in the Hybrid Boundary Element Method. *Fatigue & Fracture of Engineering Materials & Structures*,

26:151-165, 2003.
Dumont, N.A., Oliveira, M.F.F., and Aguilar, C.A., Toward a meshless formulation of the simplified hybrid boundary element method. *Book of Abstracts ICCESMM'09 - ICCES Special Symposium on Meshless & Other Novel Computational Methods*, p 21, Bistra Castle, Ljubljana, Slovenia, 2009.
Dumont, N.A., An assessment of the spectral properties of the matrix G used in the boundary element methods. *Computational Mechanics*, 22(1):32-41, 1998.
Dumont, N.A., and Oliveira, M.F.F., An expedite formulation of the boundary element method. *Abstracts of ICCES'10 – Int. Conf. on Computational & Experimental Engineering and Sciences*, Las Vegas, USA, eds. D.W. Pepper & S.N. Attluri (on CD), 2010.
Dumont, N.A., On the spectral properties of the double layer potential matrix H of the boundary element methods. *Proc. of PACAM XI - 11th Pan-American Congress of Applied Mechanics*, 6 pp on CD, Foz do Iguaçu, Brazil, 2010.
Dumont, N.A., The boundary element method revisited. *Boundary Elements and Other Mesh Reduction Methods XXXII*, ed. Brebbia, C.A., WITPress, 227-238, 2010.
Dumont, N.A., The hybrid boundary element method: an alliance between mechanical consistency and simplicity. *Applied Mechanics Reviews*, 42(11): S54-S63, 1989.
Dumont, N.A., Variationally-based, hybrid boundary element methods. *Computer Assisted Mechanics and Engineering Sciences,* 10:407-430, 2003.
Horn R.A., and Johnson C.R., *Matrix Analysis*. Cambridge University Press, 1985.
Irons B., and Ahmad S., *Techniques of Finite Elements*. Ellis Horwood Ltd., 1980.
Oliveira, M. F. F., and Dumont, N. A., Conceptual completion of the simplified hybrid boundary element method. In *Advances in Boundary element Techniques X, Proceedings of the 10th International Conference*, eds. E. J. Sapountzakis, M. H. Aliabadi, Athens, Greece, 49-54, EC, Ltd., 2009.
Oliveira, M.F.F., *Conventional, Hybrid and Simplified Boundary Element Methods*, M.Sc Thesis, PUC-Rio, Brazil, 2004.
Partridge, P.W, Brebbia, C.A., and Wrobel, L.C., *The Dual Reciprocity Boundary Element Method*, Computational Mechanics Publications, 1992.
Pian, T.H.H., Derivation of element stiffness matrices by assumed stress distribution. *AIAA J.*, 2, 1333-1336, 1964.
Qin, Q.H., *Green's Function and Boundary Elements of Multifield Materials,* Elsevier, 2007.
Reissner, E., On a variational theorem in elasticity, *Journal Math. Phys.,* 29: 90-95, 1950.
Rencis, J.J., Mann, K.C., and Urekev, T.J., The effect of essential boundary conditions on the convergence of iterative equation solvers in BEM. *Proc. of the Int. Conf. on Computational Engineering Science*, eds. S.N. Atluri, G. Yagawa and T.A. Cruse, Springer-Verlag, Vol. 2, 3068-3073, 1995.
Wagner, M., Gaul, L., and Dumont, N.A., The Hybrid Boundary Element Method in Structural Acoustics. *ZAMM - Journal of Applied Mathematics and Mechanics / Zeitschrift für Angewandte Mathematik und Mechanik*, 84(12):780-796, 2004.